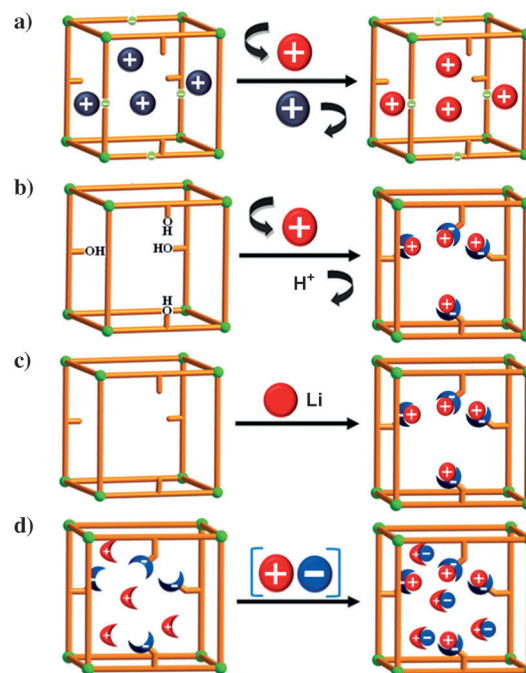


Post-Synthetic Modification of Porphyrin-Encapsulating Metal–Organic Materials by Cooperative Addition of Inorganic Salts to Enhance CO₂/CH₄ Selectivity**

Zhenjie Zhang, Wen-Yang Gao, Lukasz Wojtas, Shengqian Ma, Mohamed Eddaoudi, and Michael J. Zaworotko*

Porous metal–organic materials (MOMs) that incorporate porphyrins can combine the physicochemical properties of the porphyrin^[1,2] while retaining the permanent porosity^[3] of the MOM, thereby facilitating gas storage,^[4] separations,^[5] and luminescence.^[6] There are two established approaches to incorporate porphyrins into MOMs: the use of functionalized porphyrins as nodes or linkers,^[7] porphMOMs; selective encapsulation of porphyrins into cages, porph@MOMs.^[8] PorphMOMs are relatively well studied and their properties have been of interest in the context of gas sorption and catalysis.^[9] Porph@MOMs have been limited by the dearth of MOMs with suitable cages and until very recently there were just three examples.^[8] The use of porphyrins as structure directing agents (SDAs) to template porph@MOMs with hitherto unknown MOMs has afforded a series of porph@MOMs in which porphyrin moieties are trapped in a “ship-in-a-bottle” fashion.^[4,10]

That porph@MOMs are now readily available affords an opportunity to fine-tune their structure and properties through either pre-synthetic design or post-synthetic modification (PSM).^[11,12] PSM typically involves condensation^[11] or coordination chemistry^[12] and in effect turns MOMs that are amenable to PSM into platforms for the study of structure–function relationships. Computational and experimental studies^[13] have indicated that PSM by over-exchange with metal ions alters the affinity of a MOM for guest molecules and thereby enables improved H₂ or CO₂ uptake.^[14] PSM that introduces metal ions has been accomplished as follows: a) exchange of guest molecules or organic cations with metal ions (Scheme 1 a);^[15] b) exchange of a hydroxy proton for a Li⁺ ion



Scheme 1. Four approaches to PSM of MOMs that introduce open metal sites: a) replacement of cationic guests with metal cations; b) exchange of a hydroxy proton for a Li⁺ ion; c) chemical reduction with Li; d) cooperative addition of metal salts to anion and cation binding sites.

cation (Scheme 1 b);^[16] c) chemical reduction of a MOM with a reductive metal, such as Li (Scheme 1 c).^[17] For example, Hupp et al. reported that the incorporation of Li⁺ ions into metal–organic frameworks (MOFs) by either chemical reduction or cation exchange enhances the isosteric heats of adsorption (Q_{st}) for both H₂ and CO₂.^[16,18] However, detailed characterization of the composition and structure of such PSM materials has been hampered by the highly disordered nature of the added cations and/or the non-stoichiometric loading of the metal cations. Herein, we describe a new approach to PSM that exploits a porph@MOM with cation and anion binding sites that enable stoichiometric addition of metal salts. Specifically, immersing single crystals of a new cadmium-based porph@MOM, porph@MOM-11, into MeOH solutions of metal chloride salts leads to coordination of metal ions to the walls of the MOM and binding of Cl⁻ ions to the metalloporphyrin moieties (Scheme 1 d).

Dark green prismatic crystals of porph@MOM-11 were harvested from the reaction of biphenyl-3,4',5-tricarboxylate

[*] Z. Zhang, W.-Y. Gao, Dr. L. Wojtas, Prof. Dr. S. Ma, Prof. Dr. M. J. Zaworotko
Department of Chemistry, University of South Florida
4202 East Fowler Ave., SCA400, Tampa, FL 33620 (USA)
E-mail: xtal@usf.edu
Homepage: <http://chemistry.usf.edu/faculty/zaworotko/>
Prof. Dr. M. Eddaoudi
Chemical Science, King Abdullah University of Science and Technology
Thuwal 23955-6900 (Kingdom of Saudi Arabia)

[**] This work is supported by King Abdullah University of Science and Technology (FIC/2010/06). The microcrystal diffraction of porph-(Cl⁻)@MOM-11 (Mn²⁺) was carried at the Advanced Photon Source on beamline 15ID-B at ChemMatCARS Sector 15 (NSF/CHE-0822838 and DE-AC02-06CH11357).

Supporting information for this article is available on the WWW under <http://dx.doi.org/10.1002/anie.201203594>.

(H₃BPT),^[19] Cd(NO₃)₂·4H₂O, and *meso*-tetra(*N*-methyl-4-pyridyl) porphine tetratosylate (TMPyP) in DMF/H₂O. Colorless prismatic crystals of a compound that exhibits a different powder X-ray diffraction (PXRD) pattern were harvested when the same reaction was conducted in the absence of TMPyP (Supporting Information, Figure S1) which is indicative of a templating effect by TMPyP. Single-crystal X-ray diffraction (SCXRD) revealed that porph@MOM-11 is an anionic framework which encapsulates cationic porphyrins in alternating channels (Figure 1 a). Fig-

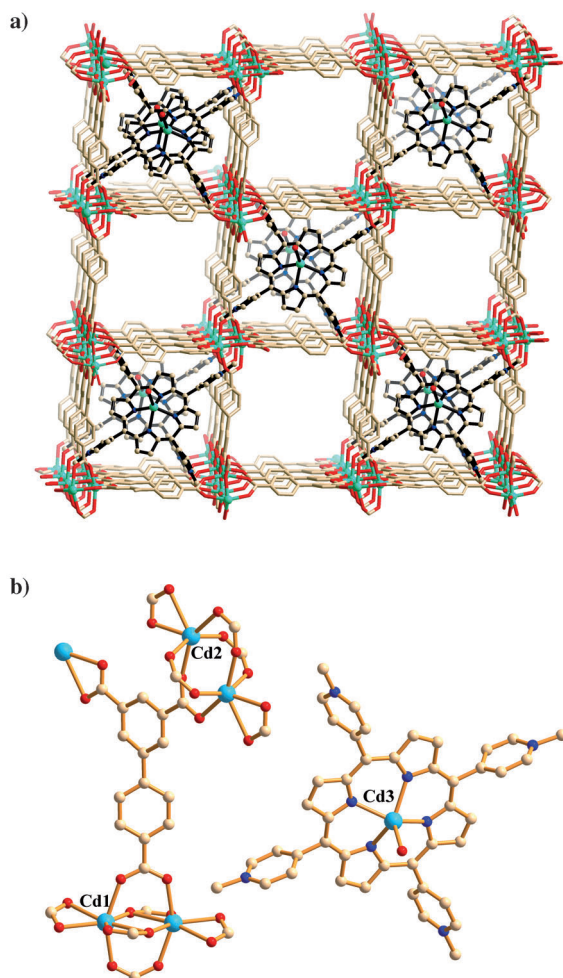


Figure 1. a) View of the crystal packing in porph@MOM-11; b) coordination environments of the Cd²⁺ ions in porph@MOM-11. Turquoise Cd, beige C, red O, blue N.

ure 1b illustrates how the framework of porph@MOM-11 contains two crystallographically independent Cd atoms (Cd1 and Cd2). Cd1 exhibits pentagonal bipyramidal geometry as a result of coordination to five carboxylate moieties, two of which are bidentate. Cd2 adopts distorted octahedral coordination geometry through six carboxylate oxygen atoms from five carboxylate moieties, one of which is bidentate. Cd–O bond distances of 2.241(4)–2.598(4) Å are consistent with expected values.^[20] Both Cd1 and Cd2 exist as dimers that serve as 6-connected, 6-c, molecular building blocks (MBBs),

[Cd₂(COO)₆]²⁻, which are not yet archived in the Cambridge Structural Database (CSD).^[21] These MBBs serve as 6-c nodes that are linked by 3-c BPT³⁻ ligands to afford a (3,6)-connected **rtl** topology net that contains channels that are based upon eight-membered rings formed from alternating 6-c and 3-c nodes (Figure S2). Blatov and Proserpio addressed (3,6)-connected nets and there is a variant which has been classified **zzz** in the RCSR database but had not yet been observed.^[22] Porph@MOM-10, which is built by the SBBs of trimetallic [Cd₃Cl₂(COO)₆]²⁻, represents the prototypal **zzz** net.^[4] Although **rtl** has the same point symbol {4.6²}₂{4².6¹⁰.8³} as **zzz**, **rtl** and **zzz** exhibit different connectivity. Figure S2 reveals how the eight-membered rings adopt 1,3-alternate geometry in **zzz** whereas they exhibit 1,2-alternate geometry in **rtl**. Porph@MOM-11 exhibits approximately 11.0 Å × 11.0 Å square channels parallel to the *a* axis (distance between opposite pore walls and subtracting the van der Waals radii). Interestingly, half of the channels are occupied by CdTMPyP moieties whereas the remaining channels are occupied by solvent molecules (DMF/H₂O). CdTMPyP cations tightly fit the **rtl** net through a series of supramolecular interactions: π···π interactions (ca. 3.5 Å) between the porphyrin arms (pyridyl groups) and phenyl groups from adjacent BPT ligands; hydrogen-bonding interactions between the terminal methyl groups of CdTMPyP cations and oxygen atoms from μ₁-η¹-η¹ chelate carboxylates (ca. 3.35 Å, C–H···O = 145°); electrostatic interactions between the anionic framework and CdTMPyP cations. The two types of channels are interconnected by windows of approximately 5.0 Å × 8.0 Å, thereby affording access to the CdTMPyP cations (Figure S3). As revealed by Figure 1 b, the Cd atom of the CdTMPyP moieties, Cd3, exhibits square-pyramidal geometry through four TMPyP nitrogen atoms and an axially coordinated solvent molecule. Cd3 lies out of the porphyrin plane with Δ*C*_β of 0.76 Å and Cd–N distances are 2.234(6) Å to 2.305(6) Å.^[23] The axial oxygen atom (Cd–O 2.322(1) Å) is weakly bonded and is amenable to replacement by ligands such as Cl⁻,^[24] therefore, the porphyrin moiety is in effect an anion binding site.

Immersion of single crystals of porph@MOM-11 in 0.125 M NaCl in MeOH for five days afforded a new phase (Figure S4), porph(Cl⁻)@MOM-11(Na⁺) that exhibits similar unit cell parameters to those of its parent porph@MOM-11. Site occupancies of the Cl, Cd, and Na ions were determined by refinement of their site occupancy factors. Chloride anions replaced the axially coordinated solvent molecules with a Cd–Cl bond of 2.555(8) Å that is consistent with reported values.^[4] As shown in Table 1, Cd1 paddlewheels bind sodium cations over two equivalent binding sites through coordination to two carboxylate oxygen atoms (Figure S5 and S6) whereas Cd2 paddlewheels do not bind to sodium cations. The Na–O(carboxylate) distances of 2.344(17) and 2.495(18) Å are within the range that would be expected (see Supporting Information).^[25] There are also cation–π interactions between sodium cations and the pyrrole groups of an adjacent CdTMPyP moiety at a distance of 3.6 Å. No metal exchange was seen in the framework or in the CdTMPyP moieties as confirmed by structure refinement and solution-state UV/Vis spectroscopy (Figure S7). The site occupancy of sodium is in

accord with atomic adsorption spectroscopy (AAS; Table S6). Porph@MOM-11 was immersed in a solution of BaCl₂ in MeOH using the same procedure as for NaCl and single crystals of porph(Cl⁻)@MOM-11(Ba²⁺) were formed. Porph(Cl⁻)@MOM-11(Ba²⁺) exhibits similar unit cell parameters to those of porph@MOM-11 and once again chloride anions replace the axially coordinated solvent molecules of the Cd porphyrin moieties. However, in porph(Cl⁻)@MOM-11(Ba²⁺) it is the Cd paddlewheels that bind to Ba²⁺ ions over two equivalent binding sites by coordination through three carboxylate oxygen atoms (Figure S8). The Ba–O(carboxylate) distances of 2.772(9), 3.067(8), and 3.192(7) Å are within expected values (see supporting information).^[26] Ba²⁺ ions in porph(Cl⁻)@MOM-11(Ba²⁺) are located within the open channels (Figure S8) and thereby reduce the pore dimensions to approximately 8.5 Å. Pore dimensions were verified by pore size distribution analysis (DFT method, Ar as analysis gas at 87 K, Figure 2). In contrast, porph(Cl⁻)@MOM-11(Na⁺) retains the same pore dimensions as porph@MOM-11, around 11.0 Å, as the Na⁺ ions coordinate to the channels that contain metalloporphyrin moieties (Figure S5).

The facile addition of Group 1 and 2 metal salts to porph@MOM-11 prompted us to study whether transition-metal cations such as Mn²⁺ and Cd²⁺ would also engage in PSM. A similar procedure to that for NaCl afforded porph-

(Cl⁻)@MOM-11(Mn²⁺) and porph(Cl⁻)@MOM-11(Cd²⁺) from MnCl₂ and CdCl₂, respectively. SCXRD revealed that they adopt the same space group (*P*-1) as porph@MOM-11 but exhibit different unit cell parameters as listed in Table 1. Table 1 also reveals that different MBBs of composition [Cd₂Mn(COO)₆(S)₄] and [Cd₃Cl(COO)₆(S)₃] are formed by rotation of one μ²-η¹η¹ carboxylate unit of the Cd1 paddlewheels to coordinate with the pendant Mn²⁺ or Cd²⁺ ions that coordinate to the walls of the open channels and reduce pore dimensions (Figure S9 and S10). The partial exchange of framework Cd atoms by Mn is in accord with our earlier observation.^[4] However, there is no metal exchange with respect to the Cd porphyrins as verified by crystallographic refinement and solution-state UV/Vis spectroscopy (Figure S7).

The partial site occupancy of added sodium (0.5), Ba (0.25), and Mn (0.5) cations can be attributed to two factors: 1) the charge balance as required by the stoichiometry of the metalloporphyrin moiety; 2) the presence of crystallographic centers of inversion. The observed site occupancies depend on the charge of added cations and whether there are one or two porphyrin moieties per unit cell (Table 1). There are two unit cell types because of the manner in which the added metals bind to the MBBs (Table 1) which means that there is only one constant amongst the four PSM structures—the Cd that is coordinated to porphyrin moieties binds to one Cl⁻ ion. The cations balance this extra negative charge. That there is full occupancy of added Cd²⁺ in porph(Cl⁻)@MOM-11(Cd²⁺) can be ascribed to an additional Cl⁻ that coordinates to a Cd²⁺ ion.

Thermogravimetric analysis (Figure S11) of porph@MOM-11, porph(Cl⁻)@MOM-11(Na⁺), porph(Cl⁻)@MOM-11(Ba²⁺), porph(Cl⁻)@MOM-11(Cd²⁺), and porph(Cl⁻)@MOM-11(Mn²⁺) indicated that they exhibit similar thermal stability with weight losses of approximately 7.8, 6.4, 10.3, 9.0, and 12.0%, respectively, below 110 °C and no further weight loss below 330 °C (following pre-exchange with methanol before TGA analysis). The Ar adsorption isotherms (Figure S12) at 87 K exhibit type I sorption behavior, which is characteristic of microporosity. BET and Langmuir surface areas for these compounds were calculated in the low-pressure region and the PSM variants exhibit comparable surface areas to that of the parent porph@MOM-11 (Table 2). However, some PSM variants exhibit higher CO₂ gravimetric uptake than their parent and all have higher CO₂ volumetric uptake despite their higher density (Table 2). To address these observations, we calculated the isosteric heats of adsorption (Q_{st}) for CO₂ from CO₂ isotherms collected at 273 K and 298 K. All the PSM variants were found to exhibit higher Q_{st} than porph@MOM-11 (Figure 3a) at both low and high loading of CO₂. Q_{st} increases of up to approximately 36% (10.9 kJ mol⁻¹) were observed in porph(Cl⁻)@MOM-11(Cd²⁺) at low loading. The increase of Q_{st} for CO₂ may be attributed to any or all of three factors: 1) smaller pore size;^[27] 2) the introduction of Cl⁻ and metal ions into the structure might enhance induced-dipole/induced-dipole interactions between the struts and CO₂;^[28] 3) the introduction of cations that bind to CO₂.^[29] The increased Q_{st} for CO₂ affects selectivity for CO₂. IAST calculations^[30] based on the

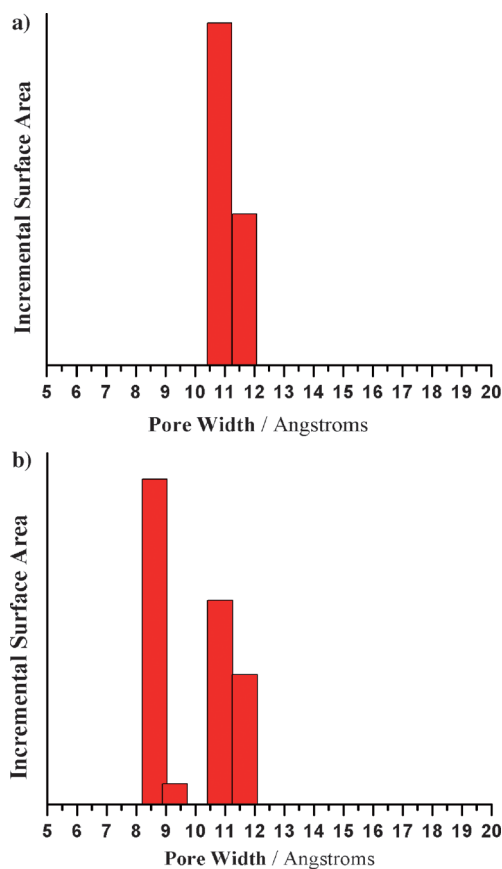


Figure 2. Pore size distribution of a) porph@MOM-11 and porph(Cl⁻)@MOM-11(Na⁺); b) porph(Cl⁻)@MOM-11(Ba²⁺).

Table 1: Structural details of the crystal structure of porph@MOM-11 and its PSM derivatives.^[a]

	Porph@MOM-11	porph(Cl ⁻)@MOM-11-(Na ⁺)	porph(Cl ⁻)@MOM-11-(Ba ²⁺)	porph(Cl ⁻)@MOM-11-(Mn ²⁺)	porph(Cl ⁻)@MOM-11-(Cd ²⁺)
Unit cell	$a = 10.027(3) \text{ \AA}$ $b = 18.420(5) \text{ \AA}$ $c = 20.577(6) \text{ \AA}$ $\alpha = 89.269(7)^\circ$ $\beta = 84.180(7)^\circ$ $\gamma = 88.402(6)^\circ$ $V = 3779.3(2) \text{ \AA}^3$	$a = 9.9445(6) \text{ \AA}$ $b = 18.539(1) \text{ \AA}$ $c = 20.288(2) \text{ \AA}$ $\alpha = 88.904(3)^\circ$ $\beta = 83.648(3)^\circ$ $\gamma = 86.713(3)^\circ$ $V = 3688(8) \text{ \AA}^3$	$a = 9.9445(6) \text{ \AA}$ $b = 18.539(1) \text{ \AA}$ $c = 20.289(1) \text{ \AA}$ $\alpha = 88.904(3)^\circ$ $\beta = 83.648(3)^\circ$ $\gamma = 86.713(3)^\circ$ $V = 3711.1(4) \text{ \AA}^3$	$a = 19.834(3) \text{ \AA}$ $b = 20.224(3) \text{ \AA}$ $c = 20.284(3) \text{ \AA}$ $\alpha = 87.480(3)^\circ$ $\beta = 64.418(3)^\circ$ $\gamma = 82.896(4)^\circ$ $V = 7282.2(1) \text{ \AA}^3$	$a = 18.3226(9) \text{ \AA}$ $b = 19.9426(8) \text{ \AA}$ $c = 21.8982(9) \text{ \AA}$ $\alpha = 67.945(2)^\circ$ $\beta = 88.290(3)^\circ$ $\gamma = 85.086(3)^\circ$ $V = 7388.8(6) \text{ \AA}^3$
Formula in unit cell	[(Cd ₄ (BPT) ₄)]·[Cd(C ₄₄ H ₃₆ N ₈)(Solvent)]·[Solvent]	[(Cd ₄ Na(BPT) ₄ (Solvent) ₃)]·[Cd(C ₄₄ H ₃₆ N ₈)(Cl)]·[Solvent]	[Cd ₄ Ba _{0.5} (BPT) ₄ (Solvent) ₃]]·[Cd(C ₄₄ H ₃₆ N ₈)(Cl)]·[Solvent]	[Cd ₈ Mn(BPT) ₈ (Solvent) ₄]]·2[Cd(C ₄₄ H ₃₆ N ₈)(Cl)]·[Solvent]	[Cd ₁₀ Cl ₂ (BPT) ₈ (Solvent) ₆]]·2[Cd(C ₄₄ H ₃₆ N ₈)(Cl)]·[Solvent]
Site occupancy ^[b]		Na 0.5	Ba 0.25	Mn 0.5	Cd 1
MBBs ^[c]					
MBBs ^[c]					
Porphyrins					
Channels incorporating metal cations					

[a] Cd (turquoise), Cl (green), Mn (pink), Na (lime), Ba (indigo). [b] Incorporated metals. [c] Cd1 is the right Cd atom, Cd2 the left Cd atom.

Table 2: Properties of porph@MOM-11 and its PSM derivatives.

Property	porph@MOM-11	porph(Cl ⁻)@MOM-11-(Na ⁺)	porph(Cl ⁻)@MOM-11-(Ba ²⁺)	porph(Cl ⁻)@MOM-11-(Cd ²⁺)	porph(Cl ⁻)@MOM-11-(Mn ²⁺)
Density [g cm ⁻³]	1.043	1.094	1.108	1.149	1.122
Increase of density	0	4.9%	6.2%	10.2%	7.6%
BET/Langmuir surface area [m ² g ⁻¹]	997/1096	965/1077	919/1020	893/995	995/1077
CO ₂ gravimetric uptake [cm ³ g ⁻¹]	90.2 and 59.4	96.9 and 65.6	92.5 and 64.3	84.5 and 54.5	96.4 and 64.4
at 273 K and 298 K (1 atm)					
CO ₂ volumetric uptake [g L ⁻¹]	184.4 and 121.6	208.2 and 141.5	201.3 and 136.7	190.2 and 122.6	211.1 and 138.3
at 273 K and 298 K (1 atm)					
Initial Qst of CO ₂ [kJ mol ⁻¹]	30.3	32.3	33.5	41.2	40.0

experimental CO₂ and CH₄ isotherms at 298 K are presented in Figure 3b and reveal that the PSM variants exhibit higher selectivity for CO₂ versus CH₄ than the parent porph@MOM-

11. Porph(Cl⁻)@MOM-11(Mn²⁺) exhibits the largest increase in selectivity (up to ca. 42% (ca. 3.0) in the low-pressure region).

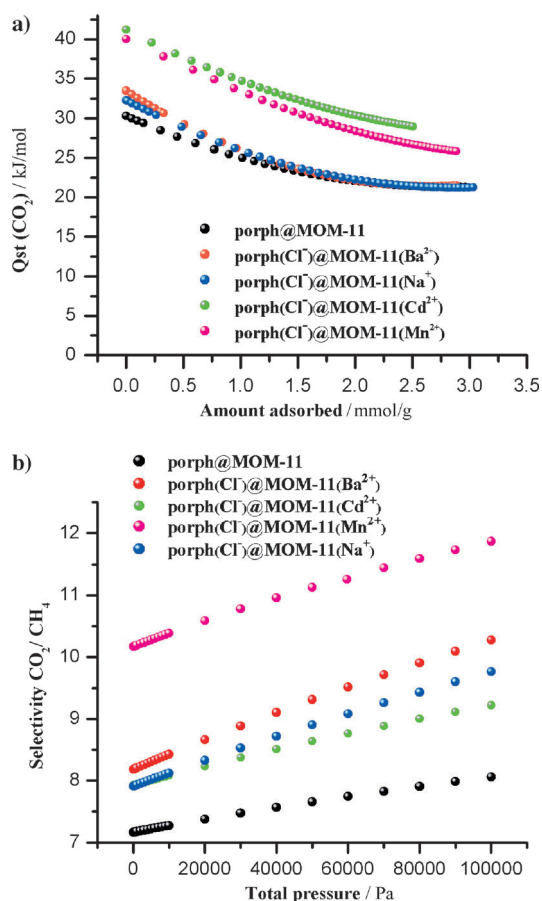


Figure 3. a) Q_{st} of CO_2 ; b) IAST calculated selectivities for adsorption from equimolar gas-phase mixtures based upon the experimentally observed adsorption isotherms of the pure gases.

In summary, a cadmium-based porph@MOM (porph@MOM-11) was synthesized using TMPyP as a template and it enabled a new strategy for PSM involving cooperative addition of metal salts by a single-crystal-to-single-crystal processes. The stoichiometric incorporation of the salts allowed a systematic study of the effect of metal cations upon gas adsorption. In the context of CO_2 , improved volumetric uptake and CO_2 versus CH_4 selectivity were observed, even with species with lower surface area and higher density than the parent porph@MOM-11.

Received: May 9, 2012

Revised: June 28, 2012

Published online: August 21, 2012

Keywords: CO_2/CH_4 selectivity · encapsulation · metal salts · metal–organic frameworks · porphyrinoids

- [1] a) H. Lu, X. P. Zhang, *Chem. Soc. Rev.* **2011**, *40*, 1899; b) I. Beletskaya, V. S. Tyurin, A. Y. Tsvadze, R. Guilard, C. Stern, *Chem. Rev.* **2009**, *109*, 1659.
[2] a) O. K. Farha, A. M. Shultz, A. A. Sarjeant, S. T. Nguyen, J. T. Hupp, *J. Am. Chem. Soc.* **2011**, *133*, 5652; b) C. Zou, Z. Zhang, X. Xu, Q. Gong, J. Li, C.-D. Wu, *J. Am. Chem. Soc.* **2012**, *134*, 87.

- [3] a) A. M. Shultz, O. K. Farha, J. T. Hupp, S. T. Nguyen, *J. Am. Chem. Soc.* **2009**, *131*, 4204.
[4] Z. Zhang, L. Zhang, L. Wojtas, P. Nugent, M. Eddaoudi, M. J. Zaworotko, *J. Am. Chem. Soc.* **2012**, *134*, 924.
[5] X.-S. Wang, L. Meng, Q. Cheng, C. Kim, L. Wojtas, M. Chrzanowski, Y.-S. Chen, X. P. Zhang, S. Ma, *J. Am. Chem. Soc.* **2011**, *133*, 16322.
[6] C. Y. Lee, O. K. Farha, B. J. Hong, A. A. Sarjeant, S. T. Nguyen, J. T. Hupp, *J. Am. Chem. Soc.* **2011**, *133*, 15858.
[7] a) K. S. Suslick, P. Bhyrappa, J. H. Chou, M. E. Kosal, S. Nakagaki, D. W. Smithenry, S. R. Wilson, *Acc. Chem. Res.* **2005**, *38*, 283; b) I. Goldberg, *Chem. Commun.* **2005**, 1243; c) B. F. Abrahams, B. F. Hoskins, D. M. Michail, R. Robson, *Nature* **1994**, *369*, 727.
[8] a) K. Ono, M. Yoshizawa, T. Kato, K. Watanabe, M. Fujita, *Angew. Chem.* **2007**, *119*, 1835; *Angew. Chem. Int. Ed.* **2007**, *46*, 1803; b) M. H. Alkordi, Y. Liu, R. W. Larsen, J. F. Eubank, M. Eddaoudi, *J. Am. Chem. Soc.* **2008**, *130*, 12639; c) R. W. Larsen, L. Wojtas, J. Perman, R. L. Musselman, M. J. Zaworotko, C. M. Vetromile, *J. Am. Chem. Soc.* **2011**, *133*, 10356; d) R. W. Larsen, J. Miksovská, R. L. Musselman, L. Wojtas, *J. Phys. Chem. A* **2011**, *115*, 11519.
[9] E.-Y. Choi, P. M. Barron, R. W. Novotny, H.-T. Son, C. Hu, W. Choe, *Inorg. Chem.* **2009**, *48*, 426.
[10] Z. Zhang, L. Zhang, L. Wojtas, M. Eddaoudi, M. J. Zaworotko, *J. Am. Chem. Soc.* **2012**, *134*, 928.
[11] K. K. Tanabe, S. M. Cohen, *Chem. Soc. Rev.* **2011**, *40*, 498.
[12] S. Cohen, *Chem. Rev.* **2012**, *112*, 970.
[13] R. Babarao, J. W. Jiang, *Ind. Eng. Chem. Res.* **2011**, *50*, 62.
[14] M. Dinca, J. R. Long, *J. Am. Chem. Soc.* **2007**, *129*, 11172.
[15] S. Yang, X. Lin, A. J. Blake, G. S. Walker, P. Hubberstey, N. R. Champness, M. Schröder, *Nat. Chem.* **2009**, *1*, 487.
[16] K. L. Mulfort, O. K. Farha, C. L. Stern, A. A. Sarjeant, J. T. Hupp, *J. Am. Chem. Soc.* **2009**, *131*, 3866.
[17] K. L. Mulfort, J. T. Hupp, *J. Am. Chem. Soc.* **2007**, *129*, 9604.
[18] Y.-S. Bae, B. G. Hauser, O. K. Farha, J. T. Hupp, R. Q. Snurr, *Microporous Mesoporous Mater.* **2011**, *141*, 231.
[19] a) A. G. Wong-Foy, O. Lebel, A. J. Matzger, *J. Am. Chem. Soc.* **2007**, *129*, 15740; b) J. K. Schnobrich, O. Lebel, K. A. Cychosz, A. Dailly, A. G. Wong-Foy, A. J. Matzger, *J. Am. Chem. Soc.* **2010**, *132*, 13941.
[20] C. I. H. Ashby, W. F. Paton, T. L. Brown, *J. Am. Chem. Soc.* **1980**, *102*, 2990.
[21] F. H. Allen, *Acta Crystallogr. B* **2002**, *B58*, 380.
[22] a) M. O'Keeffe, Reticular Chemistry Structure Resource (<http://rcsr.anu.edu.au/>); b) V. A. Blatov, D. M. Proserpio, *Acta Crystallogr. A* **2009**, *65*, 202; c) V. A. Blatov, *IUCr CompComm Newl.* **2006**, *7*, 4.
[23] D. B. Berezin, O. V. Shukhto, M. S. Reshetyan, *Russ. J. Gen. Chem.* **2010**, *80*, 518.
[24] *The Porphyrin Handbook* (Eds.: K. M. Kadish, K. M. Smith, R. Guilard), Academic Press, San Diego, **2000–2003**.
[25] J. Tao, X. Yin, R. B. Huang, L.-S. Zheng, S. W. Ng, *Acta Crystallogr. E* **2003**, *59*, m611.
[26] Y. Yokomori, K. A. Flaherty, D. J. Hodgson, *Inorg. Chem.* **1988**, *27*, 2300.
[27] J. An, N. L. Rosi, *J. Am. Chem. Soc.* **2010**, *132*, 5578.
[28] K. L. Mulfort, T. M. Wilson, M. R. Wasielewski, J. T. Hupp, *Langmuir* **2009**, *25*, 503.
[29] K. Sumida, D. L. Rogow, J. A. Mason, T. M. McDonald, E. D. Bloch, Z. R. Herm, T.-H. Bae, J. R. Long, *Chem. Rev.* **2012**, *112*, 724.
[30] Y.-S. Bae, K. L. Mulfort, H. Frost, P. Ryan, S. Punnathanam, L. J. Broadbelt, J. T. Hupp, R. Q. Snurr, *Langmuir* **2008**, *24*, 8592.